

ISSN 1996-3343

Asian Journal of
Applied
Sciences



Research Article

Dielectric Relaxation Analysis of Chemical Solid Electrolyte Lithium Aluminum Titanium Phosphate

^{1,2}Tasiu Zangina, ^{3,4}Jumiah Hassan, ^{3,4}Khamirul Amin Matori, ^{3,4}Raba'ah Syahidah Azis, ⁵Chifu Ebenezer Ndikilar and ⁶Fatin Hana Naning

¹Department of Physics, Faculty of Science, Universiti Putra Malaysia, 43400 Serdang, Selangor, Malaysia

²Department of Physics, Faculty of Science, Federal University Dutse, P.M.B. 7156 Dutse, Jigawa, Nigeria

³Department of Physics, Faculty of Science, Universiti Putra Malaysia, 43400 Serdang, Selangor, Malaysia

⁴Institute of Advanced Technology, Universiti Putra Malaysia, 43400 Serdang, Selangor, Malaysia

⁵Department of Physics, Faculty of Science, Federal University Dutse, P.M.B. 7156 Dutse, Jigawa, Nigeria

⁶Department of Basic Science and Engineering, Faculty of Agriculture and Food Science, Universiti Putra Malaysia, Bintulu Sarawak Campus, 98007 Bintulu, Sarawak, Malaysia

Abstract

Background and Objective: The study of relaxation and ionic conductivity behavior of conducting materials comes to be a significant area of research interest due to their potential application in electronic devices. The objective of the present study was to investigate the dielectric relaxation property of lithium aluminum titanium phosphate $\text{Li}_{1.5}\text{Ti}_{1.5}(\text{PO}_4)_3$ with NASICON-type structure.

Materials and Methods: The material was prepared by conventional solid state technique, while characterization was carried out using X-ray powder diffraction (XRD) and impedance spectroscopy (IS) analysis technique. The structure and phase composition of the material was indicated by XRD analysis. Temperature and frequency dependence of AC conductivity and dielectric relaxation behavior were obtained at different temperatures from 30-280°C within the frequency range of 40 Hz to 1 MHz. **Results:** The AC conductivity was observed to be frequency-independent in the low frequency region and frequency-dependent at higher frequency region (10 KHz to 1 MHz). For dielectric permittivity analysis, the dielectric constant ϵ' and dielectric loss ϵ'' were found to increase at low frequency and decrease as frequency increased at all temperatures. The calculated AC conductivity of $6.61 \times 10^{-4} (\Omega\text{m})^{-1}$ was observed at room temperature (30°C). The relaxation energy (E_a) of 0.21 eV was obtained from electrical modulus formalism. **Conclusion:** The synthesized sample $\text{Li}_{1.5}\text{Ti}_{1.5}\text{Al}_{0.5}(\text{PO}_4)_3$ indicated two relaxation processes, in each relaxation the peaks shifted to higher frequency as the measuring temperature increased.

Key words: NASICON-type, XRD, impedance spectroscopy, conductivity, dielectric relaxation

Citation: Tasiu Zangina, Jumiah Hassan, Khamirul Amin Matori, Raba'ah Syahidah Azis, Chifu Ebenezer Ndikilar and Fatin Hana Naning, 2018. Dielectric relaxation analysis of chemical solid electrolyte lithium aluminum titanium phosphate. Asian J. Applied Sci., 11: 46-55.

Corresponding Author: Tasiu Zangina, Department of Physics, Faculty of Science, Universiti Putra Malaysia, 43400 Serdang, Selangor, Malaysia
Department of Physics, Faculty of Science, Federal University Dutse, P.M.B. 7156 Dutse, Jigawa, Nigeria Tel: +2348032136356

Copyright: © 2018 Tasiu Zangina *et al.* This is an open access article distributed under the terms of the creative commons attribution License, which permits unrestricted use, distribution and reproduction in any medium, provided the original author and source are credited.

Competing Interest: The authors have declared that no competing interest exists.

Data Availability: All relevant data are within the paper and its supporting information files.

INTRODUCTION

Sodium Super Ionic Conducting materials known as NASICON-type, based on Lithium Titanium Phosphate $\text{LiTi}_2(\text{PO}_4)_3$ (LTP) are the most studied materials due to their potential application in lithium ion battery. The LTP materials belong to the family of NZP compounds known as Sodium (Na) Zirconia Phosphate. The crystal structure of the composition NZP was first reported by Alamo and Roy¹ and Hagman and Kierkegaard². The NASICON structure with the general formula $\text{AB}_2(\text{MO}_4)_3$ is made up of three dimensional network BO_6 octahedral and MO_4 tetrahedral corner-sharing with A as mobile ion in the crystal structure which occupy the interstitial sites. The conduction and interstitial networks are generated along the c-axis^{2,3}. The atoms located in the lattice structure can be substituted with suitable element in the periodic table e.g. Na can be substituted with Li, Cs, Ca or Br and Ti, Ge, Hf by Zr and Si for P except oxygen. This can form a compound with different physical and chemical behavior that can be utilized in many applications⁴.

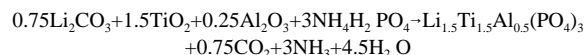
There are many reports related to the LTP system with aluminum substitution, in which majority of the reports were based on various synthesis techniques. Kotobuki and Koish reported the synthesis of Lithium Aluminum Titanium Phosphate $\text{Li}_{1.5}\text{Ti}_{1.5}\text{Al}_{0.5}(\text{PO}_4)_3$ (LATP) via sol-gel method with various aluminum sources such as $\text{Al}(\text{NO}_3)_3$ and $\text{Al}(\text{C}_3\text{H}_7\text{O})_3$ where the influence of Al sources were examined and discussed⁵. The most studied compositions in $\text{Li}_{x+1}\text{Ti}_{2-x}\text{Al}_x(\text{PO}_4)_3$ system are those with $x = 0, 0.3$ and 0.4 , but very few works were reported with composition $x = 0.5$ and also the relaxation behavior of $\text{Li}_{1.5}\text{Ti}_{1.5}\text{Al}_{0.5}(\text{PO}_4)_3$ was not fully reported.

The study of ionic conductivity and relaxation property of conducting materials becomes a remarkable area of research interest due their potential application in electronic devices⁶. A technique for analyzing the relaxation property of composite materials is the method of dielectric modulus formalism which gives opportunity to study the electric conductivity and the relaxation phenomenon of materials⁷. The present study was carried out to study the frequency and temperature dependence of ionic conductivity properties of $\text{Li}_{x+1}\text{Ti}_{2-x}\text{Al}_x(\text{PO}_4)_3$ with $x = 0.5$ in the frequency range 40 Hz to 1 MHz at different measuring temperatures from 30-280°C. The dielectric relaxation behavior of the compositions also investigated in the present study.

MATERIALS AND METHODS

The material synthesis and characterizations was carried out in Solid State Laboratory, Physics Department, Universiti

Putra Malaysia during PhD research study from 2014-2017. The NASICON-type material $\text{Li}_{x+1}\text{Ti}_{2-x}\text{Al}_x(\text{PO}_4)_3$ with stoichiometry composition $x = 0.5$ was synthesized by employing conventional solid state synthesis technique (Solid State Laboratory Physics Department, Universiti Putra Malaysia) using the raw materials Li_2CO_3 (99% Alfa Aesar), TiO_2 (99.9% Alfa Aesar), $\text{NH}_4\text{H}_2\text{PO}_4$ (98% Alfa Aesar), and Al_2O_3 (96% Strem). The chemical reaction for the synthesis as follows:



The raw materials were mixed in ethanol (as mixing agent) then ball mixed using ball mixing machine for about 24 h. The resulting mixture was dried in an oven for 6 h. The stoichiometric mixture was then heated at 700°C for about 4 h at the heating rate of 2°C/min in air. The raw materials decomposed during heating and releases H_2O , CO_2 and NH_3 as in the given chemical reaction above. The pre-sintered materials were ground and made into pellets of 11.6 mm diameter and 2.83 mm thickness (t) using uniaxial hydraulic pressing machine and finally sintered at 1100°C.

The synthesized LATP was characterized using x-ray diffraction machine (Philips X'pert diffractometer model 7602 EA Almelo. Physics Department, Universiti Putra Malaysia) with Cu K α radiation source and $\lambda = 1.5418 \text{ \AA}$. Measurement of the diffraction patterns was carried out at room temperature with 2θ ranging from 20-70°C. The data was interpreted using the database of the Inorganic Crystal Structure Database (ICSD) by employing High Score X-part plus software version 3.0 e.

Dielectric characterization on the sintered $\text{Li}_{1.5}\text{Ti}_{1.5}\text{Al}_{0.5}(\text{PO}_4)_3$ was performed using Agilent 4294A precision impedance analyzer coupled with LT furnace in the frequency range 40 Hz to 1 MHz and at different measuring temperatures from 30-280°C.

RESULTS AND DISCUSSION

The x-ray diffraction pattern XRD of the sample $\text{Li}_{1.5}\text{Ti}_{1.5}\text{Al}_{0.5}(\text{PO}_4)_3$ sintered at 1100°C was shown in Fig. 1. All the diffraction peaks were based on hexagonal axis with R-3c space group with ICSD database 98-006-9677 of NASICON-type LATP. The lattice parameters were obtained from the software after Rietveld analysis $a = 8.4999 \text{ \AA}$, $c = 20.798 \text{ \AA}$ and the unit cell volume $V = 1301.3 \text{ \AA}^3$. The calculated lattice constant and the unit cell volume were found to be in good agreement with the value already reported^{3,8}. It was observed that the lattice constant obtained

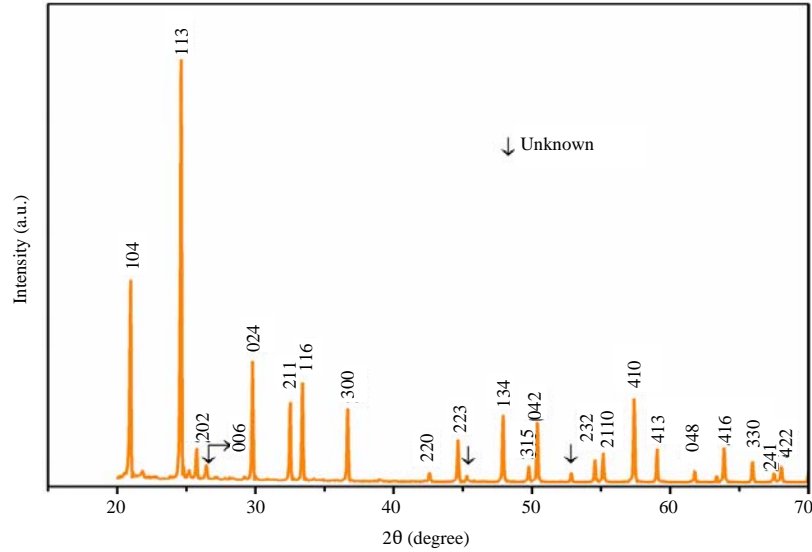


Fig. 1: X-ray diffraction pattern of the sample of $\text{Li}_{1.5}\text{Ti}_{1.5}\text{Al}_{0.5}(\text{PO}_4)_3$ sintered at 1100°C

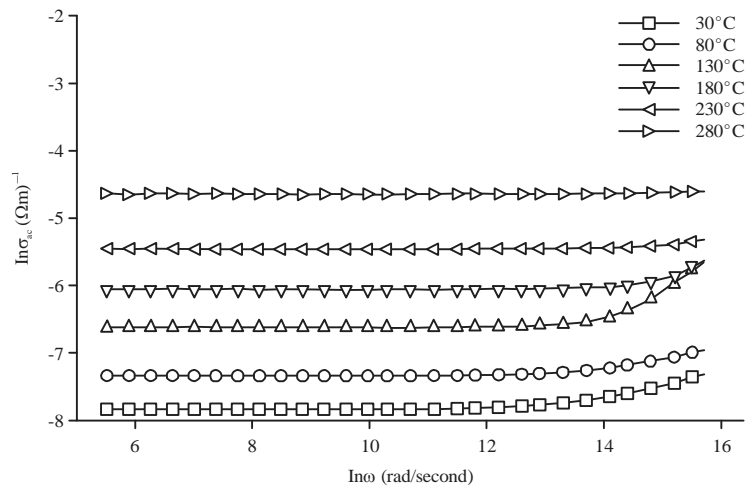


Fig. 2: Variation of AC conductivity ($\ln\sigma_{ac}$) with frequency ($\ln\omega$) of LATP at various temperatures

for the as-prepared LATP are little bit smaller than that of the un-substituted lithium titanium phosphate LTP reported⁸. This was attributed to the aluminum substitution, because aluminum ion smaller than titanium ion^{8,9}.

Variation of AC conductivity ($\ln\sigma_{ac}$) with frequency ($\ln\omega$) in rad per second at different temperatures from 30-280°C shown in Fig. 2. The AC conductivity $\sigma_{ac}(\omega)$ was calculated using Eq. 1^{10,11}:

$$\sigma_{ac}(\omega) = G(\omega) \frac{t}{A} \quad (1)$$

where, G was the measured conductance from 40 Hz to 1 MHz, t was the sample thickness (2.83×10^{-3} m) and A was the area (1.10×10^{-4} m). It was observed from the Fig. 2 that the

AC conductivity slightly increased as frequency increased. High AC conductivity was observed as measuring temperature increases which indicated the common response of ionic conductors. This was also associated with the mobility of Li^+ ion (charge carriers) in the polycrystalline composite materials at higher temperatures. Two regions were observed in all the plots, the AC conductivity was weakly dependent on frequency in the low frequency region from 40 Hz to 100 KHz (equivalent to 5.5-14 rad/second) which was associated with free charge ions present at the sample-electrode interface. The second region from 100 KHz to 1 MHz (14-15.7 rad/second) was the frequency-dependent region which was attributed to the ions trapped at high frequency region¹². The frequency dependent region exhibited the features of Almond-West universal power law Eq. 3. This region was almost temperature

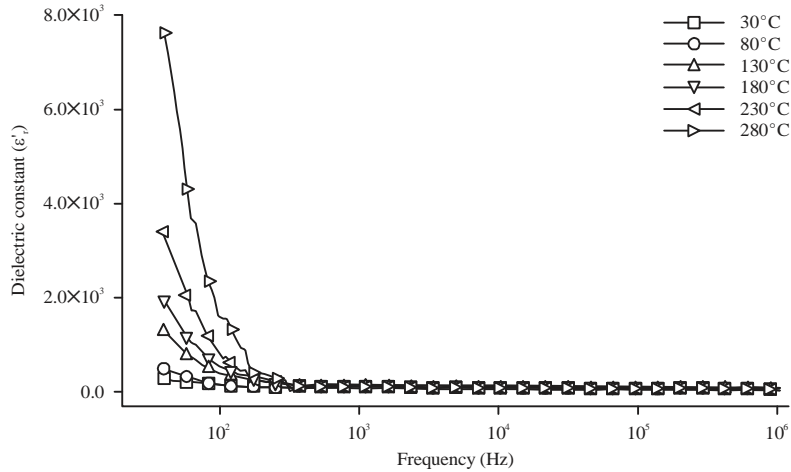


Fig. 3: Variation of dielectric constant with frequency of $\text{Li}_{1.5}\text{Ti}_{1.5}\text{Al}_{0.5}(\text{PO}_4)_3$ sintered at 1100°C at different measuring temperatures

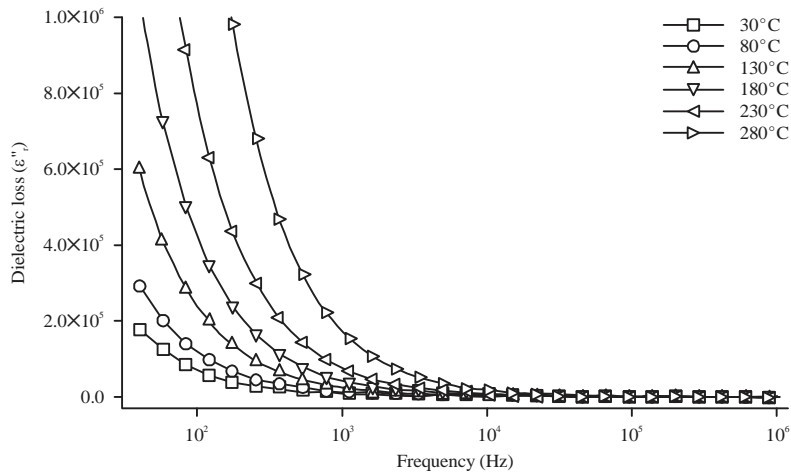


Fig. 4: Frequency dependence of dielectric loss of $\text{Li}_{1.5}\text{Ti}_{1.5}\text{Al}_{0.5}(\text{PO}_4)_3$ sintered at 1100°C at various temperatures

dependent¹³. The total conductivity $\sigma(\omega)$ comprised of DC conductivity (low frequency region) and AC conductivity (higher frequency region) described by Jonscher power law Eq. 2^{5,11}. This equation represented many-body interaction of charges and the mechanisms for the transport of ions⁶. Similarly, observed that at 280°C the conductivity was temperature dependence.

$$\sigma(\omega) = \sigma_{dc}(\omega) + \sigma_{ac}(\omega) \quad (2)$$

$$\sigma_{ac}(\omega) = A\omega^s \quad (3)$$

where, A was the constant parameter which was dependent on temperature:

$$\omega = \frac{2\pi}{\tau}$$

with τ as relaxation time and s was the frequency exponent and σ_{dc} was the DC conductivity which was observed in the low frequency region^{13,14}.

The variations of dielectric permittivity consisting of real ($\epsilon'(\omega)$) and imaginary ($\epsilon''(\omega)$) parts with frequency at different measuring temperatures from 30 – 280°C in the frequency range 40 Hz to 1 MHz were depicted in Fig. 3 and 4, respectively. Both plots showed similar trend and exhibit the behavior of ionic conducting material. It could be seen in the Fig. 3 that there was high dielectric constant ϵ' at lower frequency below 1 KHz but at higher frequency above 1 KHz to 1 MHz, dielectric constant decreases and reached a constant value. This was because the charge ions at low frequency had enough time to accumulate at the interface of the conducting regions^{12,15}. While at higher frequency the charge ions have no time to accumulate which lead to the absence of interfacial polarization. Hence, the $\epsilon'(\omega)$ tends to

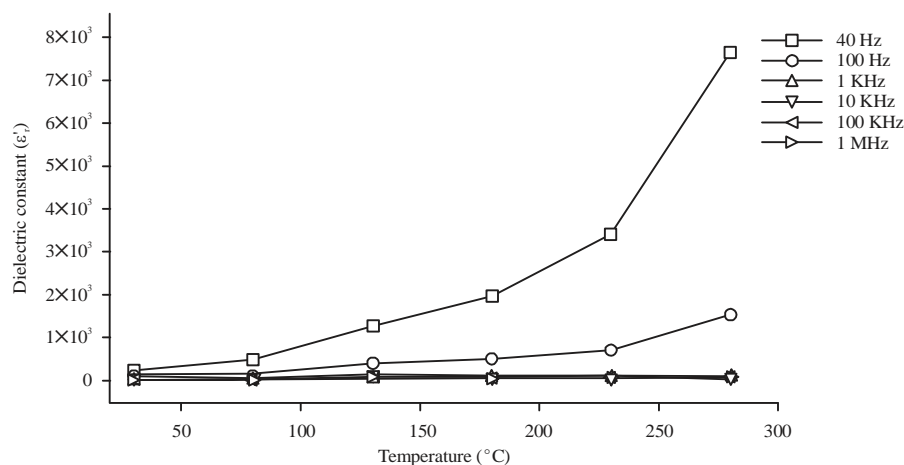


Fig. 5: Temperature dependence of dielectric constant of $\text{Li}_{1.5}\text{Ti}_{1.5}\text{Al}_{0.5}(\text{PO}_4)_3$ sintered at 1100°C at selected frequencies

reach a constant value at higher frequencies¹⁶. Electrical energy loss (dielectric loss ϵ'') was observed in Fig. 4, which showed high dielectric loss at low frequency region which was associated with migration of charge ions in the $\text{Li}_{1.5}\text{Ti}_{1.5}\text{Al}_{0.5}(\text{PO}_4)_3$ lattice. The charge ions loss energy to the lattice in form of heat during migration. But, at higher frequency the dielectric loss ϵ'' was observed to decrease. The behavior of ϵ' and ϵ'' with increasing temperatures were also observed from the plots of the Fig. 3 and 4. As measuring temperature increases, the value of ϵ' and ϵ'' also increased in the low frequency region which was associated to the thermal activation of the mobile ions.

The temperature dependence of the dielectric constant at selected frequency was illustrated in Fig. 5. The plot ϵ' was temperature-dependent in the low frequency region (40-100 Hz) but, at higher frequency region (1 KHz-1 MHz) it exhibited temperature-independent property due to the absence of space charge contribution¹⁷.

The variations of real (Z') and imaginary (Z'') parts of complex impedance with frequency at different measuring temperatures within the frequency range 40 Hz to 1 MHz of $\text{Li}_{1+x}\text{Al}_x\text{Ti}_{2-x}(\text{PO}_4)_3$ with $x = 0.5$ were shown in Fig. 6a-b, respectively. It could be seen in Fig. 6a that Z' decreased as frequency increases for all temperatures and tend to merge at 100 KHz showing the increment in ac conductivity as temperature increases. The frequency dependence of Z'' at different measuring temperatures was shown in Fig. 6b which indicated the relaxation behavior. In all the plots the values of Z'' increased to a maximum peak at lower frequency from 40 Hz to 100 KHz. The peaks of the curves exhibited systematic fall after reaching a maximum as the frequency increased to 1 MHz. Similarly, the peaks showed systematic broadening as measuring temperature increases ($30\text{-}280^\circ\text{C}$)

and shift towards higher frequency due to higher measuring temperature. This confirmed the electrical relaxation behavior of $\text{Li}_{1.5}\text{Al}_{0.5}\text{Ti}_{1.5}(\text{PO}_4)_3$ was highly temperature dependent. Furthermore, there were two relaxation processes, the first relaxation behavior was observed at lower temperatures from $30\text{-}80^\circ\text{C}$ with the same dominant charge carriers. The second relaxation process was observed at higher temperatures from $130\text{-}280^\circ\text{C}$ which was associated with another dominant charge carrier in the system. This behavior was clearly illustrated in Fig 6b and Fig. 9 which may be due to the various secondary phases and impurities located at the sample-electrode interface or probably with intrinsic nature of $\text{Li}_{1.5}\text{Ti}_{1.5}\text{Al}_{0.5}(\text{PO}_4)_3$.

The Nyquist plots of $\text{Li}_{1.5}\text{Ti}_{1.5}\text{Al}_{0.5}(\text{PO}_4)_3$ NASICON-type material at different temperatures from $30\text{-}280^\circ\text{C}$ in the frequency range 40 Hz to 1 MHz shown in Fig. 7a. Several information were deduced from the plots where the grain-interior (R_g) and grain boundary (R_{gb}) resistances were estimated and measured by carrying out equivalent circuit modeling using Nova software (version 1.11.1). The fitted Nyquist plots with two parallel RC equivalent circuits in series arrangement shown in Fig. 7b. The parameters of equivalent circuit model, grain-interior resistance (R_g), grain boundary (R_{gb}), grain-interior capacitance (C_g), grain-boundary capacitance (C_{gb}) and chi square χ^2 values (measurement accuracy) are presented and tabulated in Table 1. It can be seen from Fig. 7a that the material's conductivity is enhanced by the reduction of the semicircle diameter at higher temperatures which is attributed to the low resistance of $\text{Li}_{1.5}\text{Ti}_{1.5}\text{Al}_{0.5}(\text{PO}_4)_3$ ^{5,17,18}. The calculated resistances (R_g and R_{gb}) together with dimension of the sample were used to calculate the DC conductivities (σ_{dcg} and σ_{dcgb}) at different measuring temperatures using Eq. 4^{19,20}. It is observed from

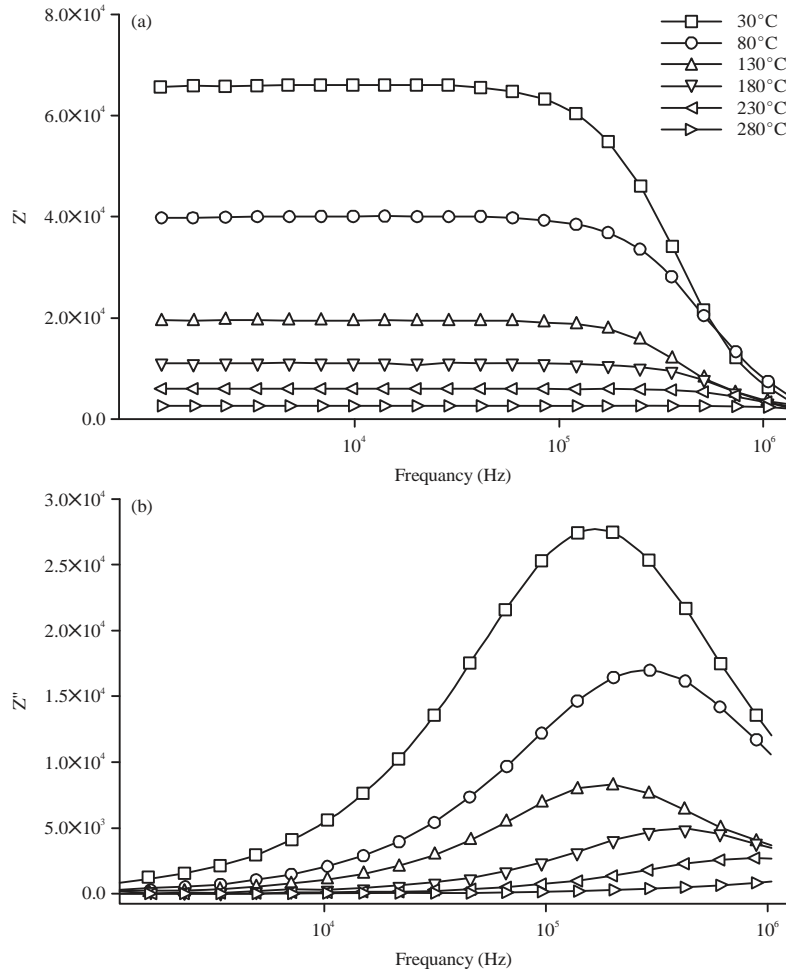


Fig. 6(a-b): Frequency dependence of LTP (a) Real part of impedance and (b) Imaginary part of the complex impedance at different measuring temperatures

Table 1: Parameters of equivalent circuit model R_{gr} , R_{gb} , C_g and C_{gb} of LTP with dimensions $t = 2.83E-03$ m $A = 1.10E-04$ m²

Temperature (°C)	R_{gr} (Ω)	R_{gb} (Ω)	C_g (F)	C_{gb} (F)	χ^2	σ_{gdc} (Ωm) ⁻¹	σ_{gbdc} (Ωm) ⁻¹
30	2.96E+04	3.42E+04	1.68E-11	4.84E-11	0.015	8.72E-04	7.55E-04
80	1.77E+04	2.14E+04	6.31E-11	1.60E-11	0.008	1.46E-03	1.21E-03
130	3.11E+03	1.63E+04	1.67E-11	5.46E-11	0.006	8.30E-03	1.58E-03
180	2.77E+03	7.42E+03	8.28E-11	6.37E-11	0.002	9.32E-03	3.48E-03
230	1.71E+03	3.96E+03	1.86E-10	3.90E-11	0.002	1.51E-02	6.52E-03
280	2.19E+02	2.48E+03	1.28E-06	2.36E-11	0.0008	1.18E-01	1.04E-02

the Table 1 that as measuring temperature increased from 30-280°C the value of measurement accuracy (χ^2) reduced which indicated the enhancement (increment of conductivity) of grain-interior σ_g and grain boundary σ_{gb} conductivity. This was associated with thermal activation energy gained by the charge carriers²¹. The measurement accuracy (χ^2) was observed to improve at higher measuring temperatures. Likewise, the grain-interior σ_g and grain boundary σ_{gb} conductivity were also observed to be enhanced at higher measuring temperatures as shown in the Table 1.

$$\sigma_{dc} = \frac{t}{RA} \quad (4)$$

The phenomenon of electrical modulus formalism was always adopted to investigate the relaxation behavior of polycrystalline material such as NASICON-type materials²². The mechanism of complex modulus formalism was useful in distinguishing grain-interior, grain-boundary conduction and the effect of electrode polarization mechanism. Another advantage of the process is that the electrode effect is always

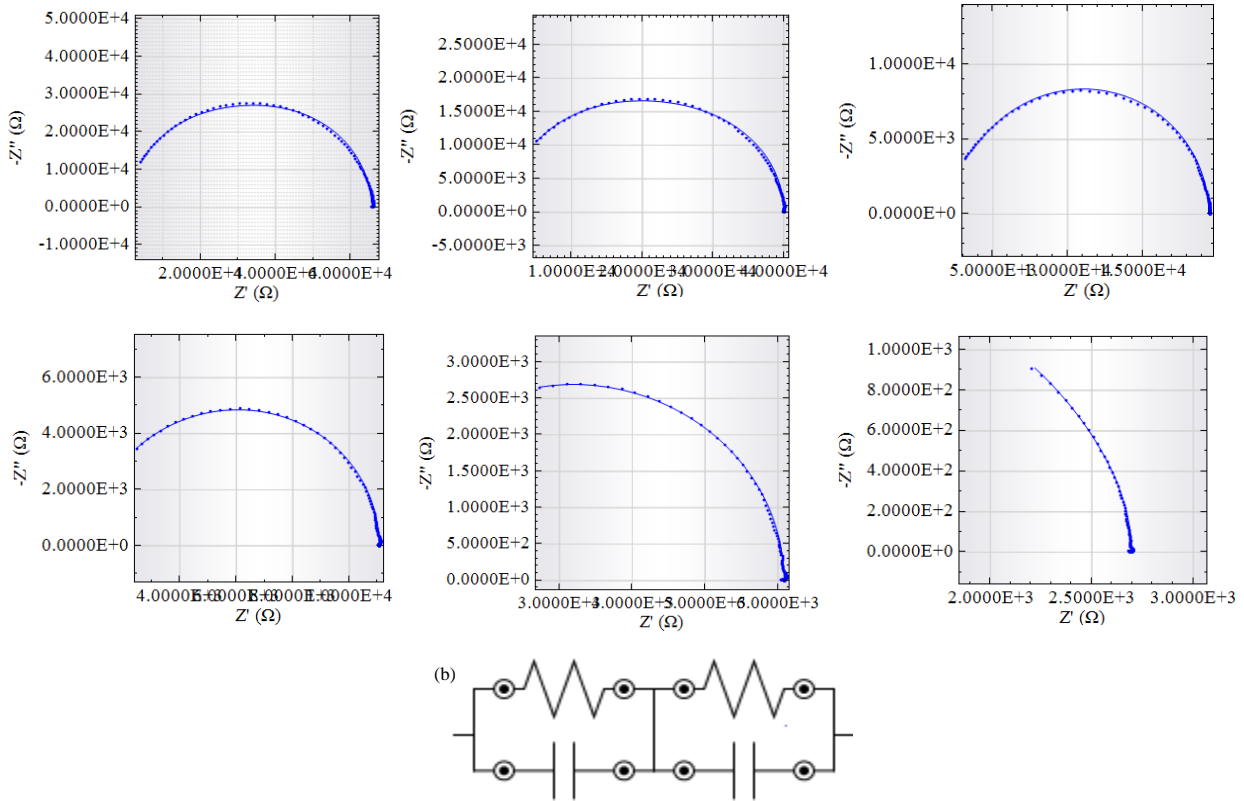


Fig. 7(a-b): (a) and (b)Nyquist plot of the complex impedance z' Vs. z'' of LATP at different temperatures

suppressed during the modulus formalism²³. The complex modulus formalism was described in terms of complex dielectric permittivity, real ϵ' and imaginary ϵ'' as shown in Eq. 5⁶.

$$M^* = \frac{1}{\epsilon^*} = M' + jM'' \quad (5)$$

Where:

$$M' = \frac{\epsilon'}{\epsilon'^2 + \epsilon''^2}$$

$$M'' = \frac{\epsilon''}{\epsilon'^2 + \epsilon''^2}$$

The variation of M spectra with frequency at various temperatures from 30-280°C in the frequency range 40 Hz to 1 MHz was depicted in Fig. 8. At lower frequency in all the plots, M' has the lowest value possibly due to the insignificant contribution of electrode effects which was probably suppressed by modulus formalism²⁴. At higher frequencies M' increased and tended to take a constant value (i.e.,

frequency-independent) above 10⁵ Hz at all measuring temperatures possibly associated with the absence of interfacial polarization which occurred due to inhomogeneity of $\text{Li}_{1.5}\text{Ti}_{1.5}\text{Al}_{0.5}(\text{PO}_4)_3$ ²⁵.

The plots of imaginary part of complex modulus M'' as a function of frequency at various temperatures was illustrated in Fig. 9. As temperature increases, the positions of the maximum peak shift towards higher frequency which confirmed the relaxation was a thermally activated process in the system²⁶. The presence of the peak in the imaginary part of the modulus spectra was associated with conductivity relaxation in the system which indicated the mobility changeover from long to short range distance. The low frequency region indicated the range at which the lithium ions can drift and hop from one site to another at a longer distance. However, at higher frequency region, the frequency range in which the ions were confined was within a potential well¹⁶ where it could only move a short distance in the potential well.

On the other hand, Fig. 9 also behaved like Fig. 6b with two relaxation processes within the frequency range 40 Hz to 1 MHz which may be due to the phase transition in the system as temperature changed from 30-280°C. The effect of

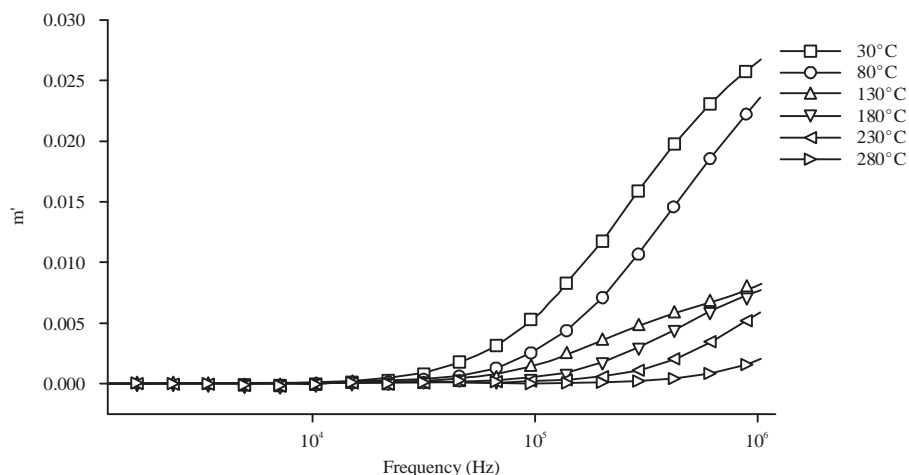


Fig. 8: Variation of real dielectric modulus (M') with frequency of LATP at various measuring temperatures

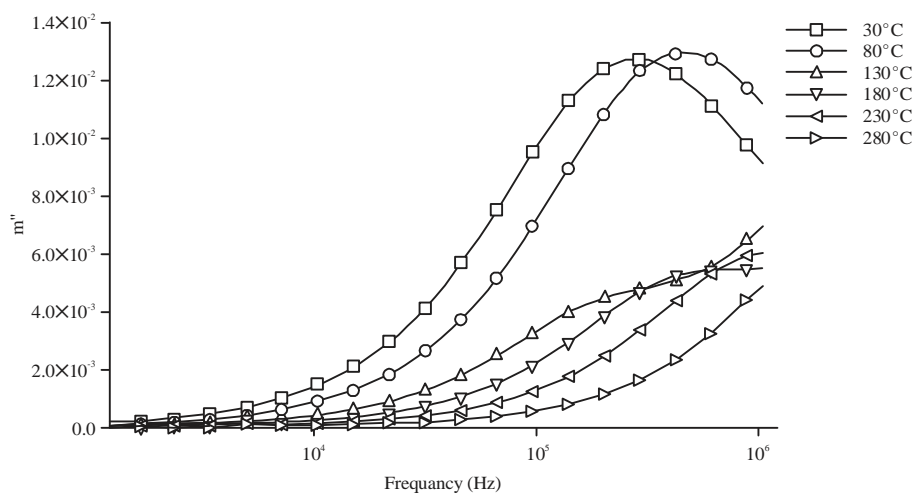


Fig. 9: Variation of imaginary part of dielectric modulus (M'') with frequency of LATP at various measuring temperatures

Table 2: Parameters of relaxation obtained from the dielectric modulus spectra for LATP

Temperature ($^{\circ}\text{C}$)	Maximum frequency f_{max} (Hz)	Relaxation frequency $\omega_{\text{max}} = 2\pi f_{\text{max}}$ (rad/second)	Relaxation time $\tau = 1/\omega_{\text{max}}$ (second)
30	2.90E+05	1.82E+06	5.49E-07
80	4.50E+05	2.83E+06	3.54E-07
130	2.18E+05	1.37E+06	7.30E-07
180	5.91E+05	3.71E+06	2.69E-07
230	8.67E+05	5.45E+06	1.84E-07
280	9.92E+05	6.23E+06	1.60E-07

two relaxations was probably attributed to the heterogenous nature of $\text{Li}_{1.5}\text{Ti}_{1.5}\text{Al}_{0.5}(\text{PO}_4)_3$ in which the properties of the sample was composed of every compound in the system. In a similar analysis,²² the sample with composition $\text{Li}_{1.3}\text{Ti}_{1.7}\text{Al}_{0.3}(\text{PO}_4)_3$ ($x = 0.3$) exhibited one relaxation at all measuring temperatures in the dielectric modulus analysis, attributed to only one type of dominant charge carriers, unlike $\text{Li}_{1.5}\text{Ti}_{1.5}\text{Al}_{0.5}(\text{PO}_4)_3$ which showed two relaxation processes.

The maximum frequency (f_{max}), at which the M'' reached maximum peak, defined the relaxation occurring in the system. The parameters of relaxation include relaxation frequency ω and relaxation time $\tau = \omega^{-1}$ were clearly tabulated in Table 2. The estimated relaxation frequency ω increased as measuring temperature increased, whereas the estimated relaxation time τ was observed to decrease with increasing temperatures. But different behaviour was observed at temperature 130°C which is due to the phase transition

occurring at different temperatures. this was clearly shown in Table 2. Based on the data obtained at higher temperatures, the electric relaxation energy for the conduction processes was found to be as low as 0.21 eV. This was regarded as activation energy of the material sample which was obtained using Arrhenius relation.

The calculated value of AC conductivity $6.61 \times 10^{-4} (\Omega\text{m})^{-1}$ at room temperature and relaxation behavior of the material (relaxation energy 0.21 eV) in the present analysis indicated that the synthesized material was suitable to be used as chemical solid state electrolyte in battery. The conductivity can be improved by using different methods rather than solid-state synthesis technique.

CONCLUSION

The dielectric analysis indicated that dielectric constant is temperature-dependent in the low frequency region (40-100 Hz) and temperature-independent at higher frequency region above 100 Hz. The plots of imaginary part of complex impedance (Z'') and modulus (M'') formalism also showed relaxation behavior of $\text{Li}_{1.5}\text{Ti}_{1.5}\text{Al}_{0.5}(\text{PO}_4)_3$. The two plots exhibited two relaxations processes, the first relaxation behavior was indicated at low temperatures from 30-80°C while the second relaxation was observed at higher temperatures above 80°C due to the different dominant charge carriers that exist in the $\text{Li}_{1.5}\text{Ti}_{1.5}\text{Al}_{0.5}(\text{PO}_4)_3$ at various temperatures.

SIGNIFICANCE STATEMENT

In the present research work, the study of relaxation behavior and conductivity properties of $\text{Li}_{1.5}\text{Ti}_{1.5}\text{Al}_{0.5}(\text{PO}_4)_3$ is elaborated. The findings help researchers to discover the relaxation behavior of the material; this is because relaxation in ionic conducting materials is one of the important tools to describe the behavior and properties of ionic transport.

ACKNOWLEDGMENTS

This study was financially supported by the Ministry of Education Malaysia through the Fundamental Research Grant Scheme (FRGS) Project No.: 01-02-14-1599FR. The authors gratefully acknowledge the Department of Physics, Faculty of Science, Universiti Putra Malaysia (UPM) for the facilities provided.

REFERENCES

1. Alamo, J. and R. Roy, 1986. Crystal chemistry of the $\text{NaZr}_2(\text{PO}_4)_3$, NZP or CTP, structure family. *J. Mater. Sci.*, 21: 444-450.
2. Hagman, L.O. and P. Kierkegaard, 1968. The crystal structure of $\text{NaMe}_2\text{IV}(\text{PO}_4)_3$; MeIV= Ge, Ti, Zr. *Acta Chem. Scand.*, 22: 1822-1832.
3. Ramaraghavulu, R. and S. Buddhudu, 2011. Analysis of structural, thermal and dielectric properties of $\text{LiTi}_2(\text{PO}_4)_3$ ceramic powders. *Ceram. Int.*, 37: 3651-3656.
4. Mariappan, C. and G. Govindaraj, 2002. Ac conductivity, dielectric studies and conductivity scaling of NASICON materials. *Mater. Sci. Eng. B*, 94: 82-88.
5. Kotobuki, M. and M. Koishi, 2013. Preparation of $\text{Li}_{1.5}\text{Al}_{0.5}\text{Ti}_{1.5}(\text{PO}_4)_3$ solid electrolyte via a sol-gel route using various Al sources. *Ceram. Int.*, 39: 4645-4649.
6. Migahed, M.D., M. Ishra, T. Fahmy and A. Barakat, 2004. Electric modulus and AC conductivity studies in conducting PPy composite films at low temperature. *J. Phys. Chem. Solids*, 65: 1121-1125.
7. Nasr, G.M. and R.M. Ahmed, 2010. AC conductivity and dielectric properties of PMMA/fullerene composites. *Mod. Phys. Lett. B*, 24: 911-919.
8. Aono, H., E. Sugimoto, Y. Sadaoka, N. Imanaka and G.Y. Adachi, 1991. Electrical property and sinterability of $\text{LiTi}_2(\text{PO}_4)_3$ mixed with lithium salt (Li_3PO_4 or Li_3BO_3). *Solid State Ionics*, 47: 257-264.
9. Arbi, K., W. Bucheli, R. Jimenez and J. Sanz, 2015. High lithium ion conducting solid electrolytes based on NASICON $\text{Li}_{1+x}\text{Al}_x\text{M}_{2-x}(\text{PO}_4)_3$ materials (M= Ti, Ge and $0 \leq x \leq 0.5$). *J. Eur. Ceram. Soc.*, 35: 1477-1484.
10. Kothari, D.H., D.K. Kanchan and P. Sharma, 2014. Electrical properties of Li-based NASICON compounds doped with yttrium oxide. *Ionics*, 20: 1385-1390.
11. Sobha, K.C. and K.J. Rao, 1995. AC conductivity and transport studies in phosphate glasses with NASICON-type chemistry. *Solid State Ionics*, 81: 145-156.
12. Shukla, N., A.K. Thakur, A. Shukla and D.T. Marx, 2014. Ion conduction mechanism in solid polymer electrolyte: An applicability of Almond-West Formalism. *Int. J. Electrochem. Sci.*, 9: 7644-7659.
13. Pradhan, D.K., R.N.P. Choudhary and B.K. Samantaray, 2008. Studies of dielectric relaxation and AC conductivity behavior of plasticized polymer nanocomposite electrolytes. *Int. J. Electrochem. Sci.*, 3: 597-608.
14. Rout, J., B.N. Parida, P.R. Das and R.N.P. Choudhary, 2014. Structural, dielectric and electrical properties of BiFeWO_6 ceramic. *J. Electron. Mater.*, 43: 732-739.

15. Funke, K., 1997. Ion transport in fast ion conductors-spectra and models. *Solid State Ionics*, 94: 27-33.
16. Savitha, T., S. Selvasekarapandian, C.S. Ramya, M.S. Bhuvaneswari and P.C. Angelo, 2007. Electrical conduction and relaxation mechanism in $\text{Li}_2\text{AlZr}(\text{PO}_4)_3$. *J. Mater. Sci.*, 42: 5470-5475.
17. Ahmadu, U., S. Tomas, S.A. Jonah, A.O. Musa and N. Rabi, 2013. Equivalent circuit models and analysis of impedance spectra of solid electrolyte $\text{Na}_{0.25}\text{Li}_{0.75}\text{Zr}_2(\text{PO}_4)_3$. *Adv. Mater. Lett.*, 4: 185-195.
18. Mustafa, N.A., S.B.R.S. Adnan, M. Sulaiman and N.S. Mohamed, 2014. Low-temperature sintering effects on NASICON-structured $\text{LiSn}_2\text{P}_3\text{O}_{12}$ solid electrolytes prepared via citric acid-assisted sol-gel method. *Ionics*, 21: 955-965.
19. Xu, X., Z. Wen, Z. Gu, X. Xu and Z. Lin, 2004. Lithium ion conductive glass ceramics in the system $\text{Li}_{1.4}\text{Al}_{0.4}(\text{Ge}_{1-x}\text{Ti}_x)_{1.6}(\text{PO}_4)_3$ ($x = 0-1.0$). *Solid State Ionics*, 171: 207-213.
20. Hodge, I.M., M.D. Ingram and A.R. West, 1976. Impedance and modulus spectroscopy of polycrystalline solid electrolytes. *J. Electroanal. Chem. Interfacial Electrochem.*, 74: 125-143.
21. Tan, F.K., J. Hassan, Z.A. Wahab and R.S. Azis, 2016. Electrical conductivity and dielectric behaviour of manganese and vanadium mixed oxide prepared by conventional solid state method. *Eng. Sci. Technol. Int. J.*, 19: 2081-2087.
22. Zangina, T., J. Hassan, K.A. Matori, R.S. Azis, U. Ahmadu and A. See, 2016. Sintering behavior, AC conductivity and dielectric relaxation of $\text{Li}_{1.3}\text{Ti}_{1.7}\text{Al}_{0.3}(\text{PO}_4)_3$ NASICON compound. *Results Phys.*, 6: 719-725.
23. Macdonald, J.R., 2009. Comments on the electric modulus formalism model and superior alternatives to it for the analysis of the frequency response of ionic conductors. *J. Phys. Chem. Solids*, 70: 546-554.
24. Bajpai, P.K. and K.N. Singh, 2011. Dielectric relaxation and AC conductivity study of $\text{Ba}(\text{Sr}_{1/3}\text{Nb}_{2/3})\text{O}_3$. *Phys. B: Condens. Matter*, 406: 1226-1232.
25. Dhankhar, S., R.S. Kundu, M. Dult, S. Murugavel, R. Punia and N. Kishore, 2016. Electrical conductivity and modulus formulation in zinc modified bismuth boro-tellurite glasses. *Indian J. Phys.*, 90: 1033-1040.
26. Wong, Y.J., J. Hassan and M. Hashim, 2013. Dielectric properties, impedance analysis and modulus behavior of CaTiO_3 ceramic prepared by solid state reaction. *J. Alloys Compd.*, 571: 138-144.